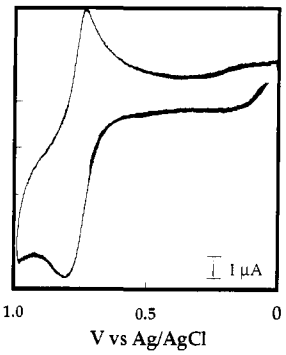

Figure 1. Cyclic voltammogram for 1 mM $[(bpy)_2Mn(O)_2Mn(bpy)_2](ClO_4)_3$ in 0.1 M phosphate buffer, pH 3.78. The potential was held at 0 V for 15 s in order to reduce all of the complex in the double layer before scanning at 50 mV/s. Other conditions were as in footnote 9.

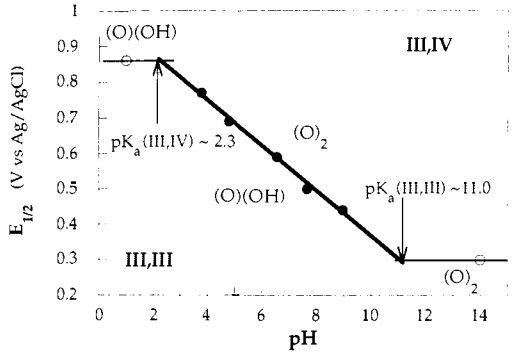

Figure 2. Pourbaix diagram for $[(bpy)_2Mn(O)_2Mn(bpy)_2](ClO_4)_3$. The closed circles are for data taken in 0.1 M phosphate buffer. The peak-to-peak splitting for all of the pH values was between 100 and 130 mV at scan rates less than or equal to 50 mV/s. The heavy line is from a linear least-squares fit to the data (R = 0.997). The open circles represent measurements made in acetonitrile; see text.

we observe good linear correlation (R = 0.998) of peak current with the square root of the scan rate.[11] These observations are also consistent with data obtained from proton-coupled reductions involving terminal oxo ligands.[8]

The pH dependence of the cyclic voltammogram shown in Figure 1 is given in Figure 2 for pH 3-9. The slope is 64 mV/pH unit, which is within experimental error of the 59 mV/pH unit required for a one-electron, one-proton couple.[11] Thus, we assign this wave to the $[(bpy)_2Mn(O)_2Mn(bpy)_2]^{3+}/[(bpy)_2Mn(O)(OH)Mn(bpy)_2]^{3+}$ III,IV/III,III couple, an assignment that is supported by the effects of electrode activation and scan rate described above.

From the measured pK_a of the III,IV dimer,[5] the potential of the pH-independent $[(bpy)_2Mn(O)(OH)Mn(bpy)_2]^{4+/3+}$ couple can be estimated to be 0.8-0.9 V from our pH-dependent data. In fact, addition of a small excess of HPF_6 to an acetonitrile solution of $[(bpy)_2Mn(O)_2Mn(bpy)_2](PF_6)_3$ gives a broad, irreversible wave with E_p = 0.86 V;[12] the same behavior is observed in 0.1 M aqueous trifluoromethanesulfonic acid.[13] Thus, we tentatively assign this wave to the $[(bpy)_2Mn(O)(OH)Mn(bpy)_2]^{4+/3+}$ III,IV/III,III couple. The open circles in Figure 2 represent this value and the known value of the irreversible $[(bpy)_2Mn(O)_2Mn(bpy)_2]^{3+/2+}$ III,IV/III,III reduction.[5,6] As shown, the pK_a of the III,III dimer can be estimated by extrapolation to the pH-dependent region. The estimated pK_a(III,III) of 11.0 is consistent with the known electrochemistry of the III,III species; a high pK_a would be expected for a complex that is unstable in nonaqueous solution but shows reversible proton-coupled behavior in aqueous solution at moderate pH. Thus, the III,III dimer is greatly stabilized by protonation of the oxo group, consistent with the observation of di-μ_2-oxo Mn^{III}_2 complexes only on the cyclic voltammetry time scale.[5,6,14]

There are a number of important biological implications of these results. First, net hydrogen atom transfer to an oxo-bridged cluster can be achieved reversibly. Second, the ability of a redox protein to regulate the effective pH in the active site may play an important role in the energetics of substrate oxidation, especially in reactions with direct proton involvement such as the oxidation of water by PS II or the oxidation of peroxide by catalase. Finally, this observation supports the idea that water oxidation in PS II may occur via binding of water or hydroxide to low-S-state manganese followed by a series of one-electron/one-proton oxidations that yield a high-valent cluster capable of coupling oxo ligands and releasing dioxygen.[1,15]

Acknowledgment. Helpful discussions with Dr. B. P. Sullivan are acknowledged. We thank the National Institutes of Health for support of this research through Grants GM-32715 and GM-40974.

(11) Bard, A. J.; Faulkner, L. R. *Electrochemical Methods*; Wiley: New York, 1980.

(12) Solutions were 1 mM in complex and 0.3 M in tetra-*n*-butylammonium hexafluorophosphate. Working electrode: polished, unactivated glassy carbon button. Auxiliary electrode: Pt wire. Reference: Ag/AgCl. Scan rate: 50-200 mV/s. The potential was determined vs Fc/Fc^+. The same results were obtained at a Pt button working electrode. The irreversible wave obtained was present for minutes but gradually decreased in intensity, consistent with other observations of complex instability at low pH.[5]

(13) The low-pH region is complicated by irreversibility and by complex instability.[5] The high-pH region is difficult to investigate, owing to numerous chemical and electrochemical factors that have been discussed: McHatton, R. C.; Anson, F. C. *Inorg. Chem.* **1984**, *23*, 3935, and Roecker, L.; Kutner, W.; Gilbert, J. A.; Simmons, M.; Murray, R. W.; Meyer, T. J. *Inorg. Chem.* **1985**, *24*, 3784.

(14) (a) Hagen, K. S.; Armstrong, W. H.; Hope, H. *Inorg. Chem.* **1988**, *27*, 967. (b) A recent report has demonstrated the use of a sterically encumbering ligand to force the formation of a di-μ_2-oxo Mn^{III}_2 complex: Goodson, P. A.; Hodgson, D. J. *Inorg. Chem.* **1989**, *28*, 3606.

(15) Gilbert, J. A.; Eggleston, D. S.; Murphy, W. R., Jr.; Geselowitz, D. A.; Gersten, S. W.; Hodgson, D. J.; Meyer, T. J. *J. Am. Chem. Soc.* **1985**, *107*, 3855.

Separate Pathways for Oxygenate and Hydrocarbon Synthesis in the Fischer-Tropsch Reaction

Douglass Miller and Martin Moskovits*

Department of Chemistry, University of Toronto Toronto, Ontario M5S 1A1, Canada

Received July 5, 1989

Fischer-Tropsch synthesis produces both hydrocarbon and oxygenated products (oxygenates) by reducing CO with hydrogen on a suitable catalyst, among which supported iron, cobalt, and rhodium are examples. Recently we have carried out Fischer-Tropsch reactions on a potassium-promoted supported-iron catalyst using perdeuterated ethylene as an additive to the H_2/CO feed. This was done as a part of a study to investigate the special role that ethylene is claimed to have in the Fischer-Tropsch process, as suggested, in part, by the low concentration of ethylene that is often observed in the products of this reaction.[1] The reaction products were subjected to scrupulous GC-CIMS analysis in order

(1) Smith, D. F.; Hawk, C. O.; Golden, P. L. *J. Am. Chem. Soc.* **1930**, *52*, 3221. Gibson, E. J.; Clarke, R. W. *J. Appl. Chem.* **1961**, *11*, 293. Pichler, H.; Schulz, H.; Elstner, M. *Brennst.-Chem.* **1967**, *48*, 78. Kibby, C. L.; Pannell, R. B.; Kobylinski, T. P. *Prepr.—Am. Chem. Soc., Div. Pet. Chem.* **1984**, *29*, 113. Pichler, H.; Schulz, H. *Chem.-Ing.-Tech.* **1970**, *42*, 1162. Hall, W. K.; Kokes, R. J.; Emmett, P. H. *J. Am. Chem. Soc.* **1960**, *82*, 1027. Molina, W.; Perrichon, V.; Sneeden, R. P. A.; Turlier, P. *React. Kinet. Catal. Lett.* **1980**, *13*, 69. Dwyer, D. J.; Somorjai, G. A. *J. Catal.* **1979**, *56*, 249. Barrault, J.; Forquy, C.; Perrichon, V. *J. Mol. Catal.* **1982**, *17*, 195. Satterfield, C. N.; Huff, G. A.; Summerhayes, R. J. *J. Catal.* **1983**, *80*, 486. Ekerdt, J. G.; Bell, A. T. *J. Catal.* **1980**, *62*, 19. Kellner, C. S.; Bell, A. T. *J. Catal.* **1981**, *70*, 418. Kobori, Y.; Yamasaki, H.; Naito, S.; Onishi, T.; Tamaru, K. *J. Chem. Soc., Faraday Trans. 1* **1982**, *78*, 1473. Morris, S. R.; Hayes, R. B.; Wells, P. B.; Whyman, R. J. *J. Catal.* **1985**, *96*, 23.

0002-7863/89/1511-9250$01.50/0

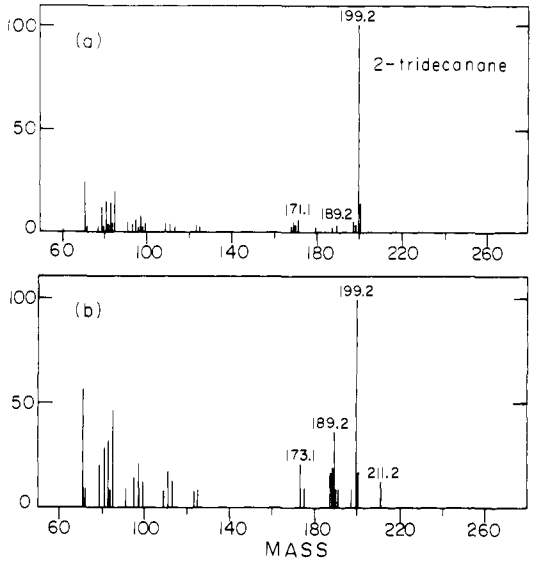

Figure 1. CIMS spectrum of 2-tridecanone ($C_{13}H_{26}O$) obtained from GC-separated products of a Fischer–Tropsch synthesis: (a) with C_2H_4 added to the CO/H_2 feed gas; (b) with C_2D_4 added to the CO/H_2 feed gas.

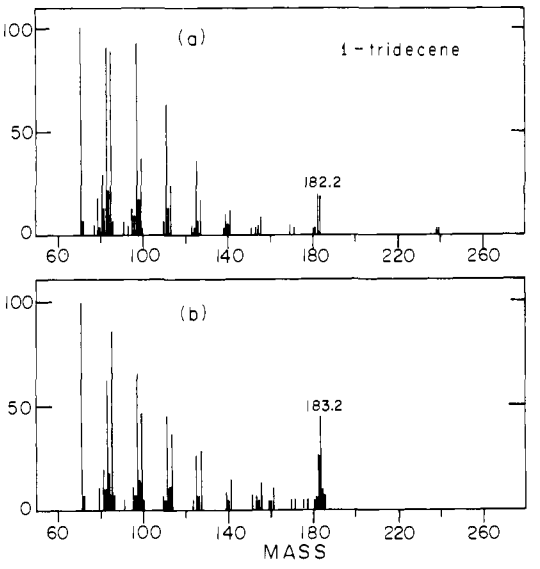

Figure 2. CIMS spectrum of 1-tridecene ($C_{13}H_{26}$) obtained from GC-separated products of a Fischer–Tropsch synthesis: (a) with C_2H_4 added to the CO/H_2 feed gas; (b) with C_2D_4 added to the CO/H_2 feed gas.

to investigate the distribution of deuterium in the Fischer–Tropsch products. We discovered that the deuterium from the deuterated ethylene was incorporated in the alkanes and alkenes almost entirely as D_2 units. (This result will be discussed in detail in another publication.[2]) The oxygenates, on the other hand, were found to have no deuterium incorporated. Examples are shown in Figure 1a,b. The prominent mass peak for the 2-tridecanone is expected to occur at m/e 199.2. The mass spectra of 2-tridecanone obtained when syngas streams were seeded with C_2H_4 and C_2D_4 are found to be identical within experimental error, indicating that there was no deuterium incorporation. By contrast, the spectrum of the 1-tridecene (Figure 2b) showed prominent mass peaks at m/e 184 and 185, precisely where one would expect them to occur if two deuteriums originating from C_2D_4 were incorporated (the 185 mass peak, for example, is due to a molecule having the formula $C_{13}H_{24}D_2$ to which one more H atom has been added in the predominant chemical ionization process occurring with olefins.) The observed ratio of deuterated to nondeuterated hydrocarbon is only consistent with a process in which both deuterium atoms are incorporated in a single step.[2] This presumably suggests that the deuterium is introduced into the hydrocarbon chain either as CD_2 or as C_2D_2. The mass peaks at 184 and 185 were absent when C_2H_4 was used in the feed stream in place of C_2D_4 during the CO hydrogenation reaction (Figure 2a).

The most plausible implication of this observation is that the oxygenates and the alkane/alkenes are synthesized on different portions of the catalyst's surface, with the oxygenates being produced on a surface phase on which ethylene either does not chemisorb at all or, at least, does not adsorb dissociatively with loss of deuterium. The alkanes and alkenes, on the other hand, are synthesized on a part of the catalyst surface where the ethylene does adsorb with loss of deuterium, and the resulting ethylenic fragment participates in one way or another in hydrocarbon formation. The most likely scenario is that oxygenates are formed almost exclusively on iron oxide (or perhaps iron carbide) portions of the catalyst while alkanes and alkenes are produced predominantly on metallic surface phases. Chain growth on both phases takes place, presumably by addition of CH_x units that are generated primarily on the metallic phase and then migrate to the oxide patches as well. This explanation is consistent with the suggestion made by several workers that oxygenates form by the insertion or incorporation of *undissociated* CO into the growing hydrocarbon chain during the CO hydrogenation reaction.[3] The CO dissociation rate on the oxide patches is lower than on the metal portions of the catalyst; hence the residence time of undissociated CO would be longer and the likelihood of molecular CO incorporation into the hydrocarbon chains growing on the oxide patches would be greater. Contrariwise, one expects ethylene to chemisorb and CO to dissociate on the metallic iron portions, in keeping with our observation that ethylene is not incorporated into oxygenates and our conclusion regarding the separate formation of oxygenates and hydrocarbons.

A Mössbauer analysis of the potassium-promoted iron catalysts prior to and after CO hydrogenation for 24 h confirmed the presence of iron and iron oxide on the catalyst.[4] The fresh catalyst was found to contain α-Fe (31%), and either two forms of Fe_2O_3 or Fe_2O_3 occupying two distinct sites in the catalyst, while the spent catalyst comprised α-Fe and an iron carbide.

Experimental Procedures. Iron catalysts employed in the ethylene incorporation reactions were prepared by electrochemical techniques.[5] Aluminum foil (Alcan 99.99%, 0.025-mm thickness) was ultrasonically degreased and etched in NaOH prior to anodization at 20 V dc in 0.87 M H_3PO_4 for 30 min in order to generate porous aluminum oxide on its surface. Lead foil was used as the cathode in the anodization process. A solution of 120 g/L $FeSO_4 \cdot 7H_2O$, 45 g/L H_3BO_3, and 0.5 g/L ascorbic acid was used in the iron electrodeposition. An ac voltage of 25 V was applied at a frequency of 200 Hz for 7 min to effect iron electrodeposition into the porous aluminum oxide support. TEM analysis showed that iron metal was incorporated into the pores in this electrolytic step. The catalysts were pretreated with potassium carbonate to a 2.0 wt % potassium content prior to the ethylene addition reactions. The iron content was 7.0% by weight of total catalyst sample, including unoxidized aluminum, and the specific metal area was 2.5 m^2/g.

Ethylene and deuterated ethylene incorporation experiments were performed at 330 °C and 6.8 atm. The foil catalyst was cut into approximately 5 mm × 5 mm coupons, and 5.15 g of catalyst was loaded into the continuous plug-flow reactor. Flow rates of 5.89 mL/min of H_2, 3.11 mL/min of CO, and 0.29 mL/min of C_2H_4/C_2D_4 were maintained with Matheson mass flow controllers. Helium was added as diluent (40 mL/min) but

(2) Moskovits, M.; Miller, D. Unpublished.

(3) Biloen, P.; Sachtler, W. M. H. *Adv. Catal.* **1981**, *30*, 165. Dictor, R. A.; Bell, A. T. *J. Catal.* **1986**, *97*, 121. Rofer-DePoorter, C. K. *Chem. Rev.* **1981**, *81*, 447. Takeuchi, A.; Katzer, J. R. *J. Phys. Chem.* **1981**, *85*, 937. Takeuchi, A.; Katzer, J. R. *J. Phys. Chem.* **1982**, *86*, 2438. Biloen, P.; Helle, J. N.; Sachtler, W. M. H. *J. Catal.* **1979**, *58*, 95. Ponec, V.; Van Barneveld, W. A. *Ind. Eng. Chem. Prod. Res. Dev.* **1979**, *18*, 268.

(4) Miller, D.; Moskovits, M.; Montano, P. Unpublished.

(5) Miller, D.; Moskovits, M. *J. Phys. Chem.* **1988**, *92*, 6081.

did not affect the catalyst activity. Reactions were carried out for 24 h in order to collect a sufficient quantity of gasoline and diesel range products for the GC–CIMS product analysis. The C_5–C_{16} hydrocarbons and oxygenates were analyzed on a Hewlett-Packard (Model 5280) gas chromatograph equipped with an OV-101 capillary column. A VG Analytical mass spectrometer coupled to the GC was employed in the product identification. Isobutane was the reagent gas in the CIMS analysis.

Acknowledgment. We are grateful to the NSERC and the Connaught Fund for financial support.

Registry No. CO, 630-08-0; potassium, 7440-09-7; iron, 7439-89-6.

A Conserved Residue of Cytochrome P-450 Is Involved in Heme-Oxygen Stability and Activation

Susan A. Martinis, William M. Atkins,† Patrick S. Stayton, and Stephen G. Sligar*

Departments of Biochemistry and Chemistry
University of Illinois
Urbana, Illinois 61801

Received August 28, 1989

The cytochrome P-450 monooxygenase systems have received substantial attention due to their unique spectral and chemical properties.[1,2] Of particular interest are the precise chemical mechanisms involved in the binding and activation of atmospheric dioxygen and the subsequent functionalization of an unactivated carbon substrate.[3,4] We now report the first demonstration of a particular active site feature of cytochrome P-450 that is essential for efficient reduction and activation of molecular dioxygen, yet is independent of the substrate binding and spin-state equilibria processes. This has been accomplished by site-directed mutagenesis of threonine 252, a residue conserved among all known P-450 sequences, to an alanine (T252A),[5] in the active site of the *Pseudomonas* cytochrome P-450$_{cam}$.

Although the individual cytochrome P-450 isozymes demonstrate marked differences in their substrate specificity,[6] predictions based on amino acid sequence analysis indicate that they share several conserved structural features.[7-9] In particular, a long proximal α-helix exhibits strong homology throughout a diverse cross section of the P-450s. The high-resolution X-ray crystal structure of cytochrome P-450$_{cam}$[10] and molecular modeling studies[10-13] suggest that the juxtaposition of oxygen and substrate is controlled by specific residues in this helix. Specifically, the I-helix contains a region of local deformation of the normal helical structure arising from a direct hydrogen bond between the peptidyl carbonyl of G248 to the side-chain hydroxyl group of T252 rather than the expected peptidyl nitrogen of the threonine residue. This unique hydrogen bond, combined with other hydrogen bonds and ion-pair interactions, produces a "kink" in the helix directly adjacent to the active site and heme iron. In addition, this defined structure contains a hydrogen-bonding network which results in the presence of protein-sequestered, ordered water molecules directly adjacent to the oxygen binding pocket. This network of hydrogen bonds may conceivably provide a source of protons to stabilize a negative charge associated with the various reduced states of oxygenated P-450.[10]

Our mutation of the conserved threonine residue to an alanine yields a stable holoprotein which is expressed in *Escherichia coli*.[14,15] The purified protein displays optical and ferric EPR

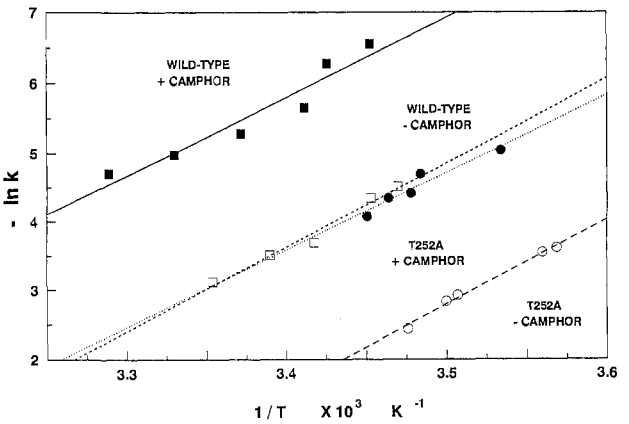

Figure 1. Comparison of substrate-free and -bound autoxidation rates of T252A and wild-type P-450$_{cam}$. Data points are denoted as follows: ■, substrate-bound wild-type; □, substrate-free wild-type; ●, substrate-bound T252A; ○, substrate-free T252A. Reactions were conducted in 700 μL of 50 mM Tris buffer, pH 7.4, 150 mM KCl, 4 mM EDTA, 0.5 μM proflavin, and 15 μM wild-type or T252A mutant. Camphor was 800 μM in the substrate-bound states. Autoxidation rates, k (s^{-1}), were measured as described.[10]

Table I. Stoichiometry of Camphor Metabolism

	wild-type (%)	T252A (%)
NADH consumption[a]	100 ± 1	100
5-*exo*-hydroxycamphor[b]	100 ± 1	5 ± 2
H_2O_2[c]	0	51 ± 2
"oxidase" water production[c]	0	22
5-*exo*-hydroxycamphor from H_2O_2-supported hydroxylation[d]	100 ± 1	16 ± 3

[a] NADH consumption was measured at 25 °C by the decrease in absorbance at 340 nm. Reaction mixtures contained 0.35 μM P-450$_{cam}$ or T252A, 2.4 μM putidaredoxin reductase, 10.6 μM putidaredoxin, 600 nmol of NADH, 150 mM KCl, 50 mM Tris, pH 7.4, and 600 nmol of camphor in a total volume of 500 μL. [b] A 500-μL reaction volume containing 50 mM Tris, pH 7.4, 150 mM KCl, 1 μmol of camphor, 4.4 μM putidaredoxin, 2 μM putidaredoxin reductase, 1 μM P-450$_{cam}$ or T252A, and 500 nmol of NADH was incubated for 15 min; 10 nmol of 3-*endo*-bromocamphor was added as an internal standard, and the solution was extracted with 1.5 mL of CH_2Cl_2, concentrated, and analyzed by gas chromatography as described.[15,26] [c] For experimental details, see: Atkins, W. M.; Sligar, S. G. *Biochemistry* **1988**, *27*, 1610–1616. [d] A reaction containing 20 μM P-450$_{cam}$ or T252A, 1 mM camphor, 50 μmol of H_2O_2, and 50 mM KP_i, pH 7.0 was halted after 10 min by the addition of $NaHSO_3$. Extraction of product and analysis were carried out as described.[15,26]

* To whom reprint requests should be addressed.
† Present address: Department of Chemistry, The Pennsylvania State University, University Park, PA 16802.

(1) Ortiz de Montellano, P. R., Ed. *Cytochrome P-450: Structure, Mechanism, and Biochemistry*; Plenum Press: New York, 1986.
(2) Griffin, B. W.; Peterson, J. A.; Estabrook, R. W. In *The Porphyrins Vol. VII*; Dolphin, D., Ed.; Academic Press: New York, 1979; pp 333–375.
(3) White, R. E.; Coon, M. J. *Annu. Rev. Biochem.* **1980**, *49*, 315–356.
(4) Sligar, S. G.; Gelb, M. H.; Heimbrook, D. C. *Xenobiotica* **1984**, *14*, 63–86.
(5) Mutations are designated by a single-letter abbreviation of the wild-type amino acid, its position number in the polypeptide chain, and the single letter abbreviation of the resultant mutant amino acid. For example, T252A represents a protein where threonine at position 252 is changed to an alanine residue.
(6) Miwa, G. T.; Lu, A. Y. H. In *Cytochrome P-450: Structure, Mechanism, and Biochemistry*. Ortiz de Montellano, P. R., Ed.; Plenum Press: New York, 1986; pp 77–88.
(7) Black, S. D.; Coon, M. J. In *Cytochrome P-450: Structure, Mechanism, and Biochemistry*; Ortiz de Montellano, P. R., Ed.; Plenum Press: New York, 1986; pp 161–216.
(8) Nebert, D. W.; Gonzalez, F. J. *Annu. Rev. Biochem.* **1987**, *56*, 945–993.
(9) Nelson, D. R.; Strobel, H. W. *J. Biol. Chem.* **1988**, *263*, 6038–6050.
(10) Poulos, T. L.; Finzel, B. C.; Howard, A. J. *J. Mol. Biol.* **1987**, *195*, 687–700.
(11) Phillips, S. E. *J. Mol. Biol.* **1980**, *142*, 531–554.
(12) Jameson, G. B.; Molinar, F. S.; Ibers, J. A.; Collman, J. P.; Brauman, J. I.; Rose, E.; Suslick, K. S. *J. Am. Chem. Soc.* **1978**, *100*, 6769–6770.
(13) Jameson, G. B.; Rodley, G. A.; Robinson, W. T.; Gagne, R. R.; Reed, C. A.; Collman, J. P. *Inorg. Chem.* **1978**, *17*, 850–857.

0002-7863/89/1511-9252$01.50/0